

Multi-level 3D VSP travel time inversion in VTI media, Weyburn Field, Canada

Ludmila Adam¹, Kasper van Wijk², and Thomas L. Davis²

¹ Reservoir Characterization Project, Colorado School of Mines

² Center of Wave Phenomena, Colorado School of Mines

Summary

A 12-level 3D vertical seismic profile (VSP) is acquired as part of Weyburn Project with of Reservoir Characterization Project (RCP) at Colorado School of Mines. Travel times from direct arrivals of compressional sources are used to invert for Thomsen's parameters for a transversely isotropic with a vertical symmetry axis (VTI) media. Near offsets are used to estimate the vertical travel time and normal moveout (NMO) velocity, while the non-hyperbolic moveout of all offsets are fitted to estimate the horizontal velocity. ϵ and δ parameters are estimated from these velocities. A sensitivity and error analysis on the parameters that control the non-hyperbolic moveout equation is performed.

Introduction

RCP is characterizing a carbonate reservoir that is undergoing CO₂ and water injection since 2000. The goal is to monitor the movement of the CO₂, changes in physical properties of the rocks and to analyze the anisotropic symmetry of the medium through time-lapse 9C 3D surface seismic. Characterization of the overburden with a 3D VSP study allows us to make inferences at the reservoir level with greater accuracy. A 9C 3D VSP was acquired with 12 levels ranging from 1232 m to 1397 m at 15 m intervals, over an area of 9 km², using 1363 shot points and having maximum offsets of 2200 m. Only the overburden is studied, as the inversions are based on direct travel times to each receiver, and the deepest receiver is just above the reservoir. The analyzed travel times were picked on tilted receivers, where the P-wave energy is maximized on the vertical component. This maximization is done making use of the horizontal components of the receiver. Receivers at 1262 m and 1352 m had no response on their horizontal components, thus the travel times were not picked for those depths. The inversion of the receivers was very similar in behavior from one another.

Estimation of anisotropic medium parameters at the reservoir level and the overburden is important to image seismic data, characterize the reservoir, and to study time changes of these parameters at a producing field. We estimate anisotropic parameters using the 3D VSP. The research is geared toward estimating these parameters from travel times of direct arrivals using P, SV and SH waves, but here we analyze the results for P-wave data only. However, shear-wave data will be presented in the near future.

Grechka and Tsvankin (1998) show a modification to the theory behind non-hyperbolic moveout. They show numerical results and invert for Thomsen's parameters, via estimates of the NMO and horizontal velocity. They also invert travel times for one receiver position in a 3D VSP at Vacuum Field, New Mexico. This case study with larger offset-to-depth ratio (3.2 compared to 2.7), multiple receivers and better data quality allows for a more detailed study of the anisotropic parameters (a different approach on error analysis) and their resolution.

Theory

Adam and Mattocks (2002) interpreted the overburden as a VTI media. In this case, the δ parameter is related to NMO (V_{nmo}) and the vertical velocity (V_0) via (Thomsen, 1986):

$$\delta = \frac{V_{nmo,p}^2 - V_{0,p}^2}{2V_{0,p}^2}. \quad (1)$$

Laboratory studies show that overall shales produce positive values of δ (Wang, 2002), while thin layering usually gives negative δ .

The definition of ϵ (Thomsen, 1986) is

$$\epsilon = \frac{V_{hor,p}^2 - V_{0,p}^2}{2V_{0,p}^2}. \quad (2)$$

Estimation of both δ and ϵ make use of the vertical velocity. These were previously obtained from the inversion of travel times for the near offset VSP using the L-curve method (Van Wijk et al., 2002; Adam, 2001). So, to estimate ϵ and δ we need the NMO and horizontal velocities.

Grechka and Tsvankin (1998) derived the non-hyperbolic moveout equation:

$$t^2(x) = t_0^2 + \frac{x^2}{V_{nmo}^2} - \frac{(V_{hor}^2 - V_{nmo}^2)x^4}{V_{nmo}^2(t_0^2 V_{nmo}^4 + C V_{hor}^2 x^2)}, \quad (3)$$

where, t is the travel time (data), t_0 is the vertical one-way travel time (for VSP data), and x is the source-receiver offset. C is an empirical constant, shown to be $C=1.2$ for a single horizontal layer (Grechka and Tsvankin, 1998), but for layered media the C value might differ. Large offsets show a trade-off between V_{nmo} and V_{hor} , while near offsets are dominated by V_{nmo} . As a rule of thumb, near offsets mean source-receiver offsets less than half the receiver depth.

3D VSP travel time inversion in VTI media

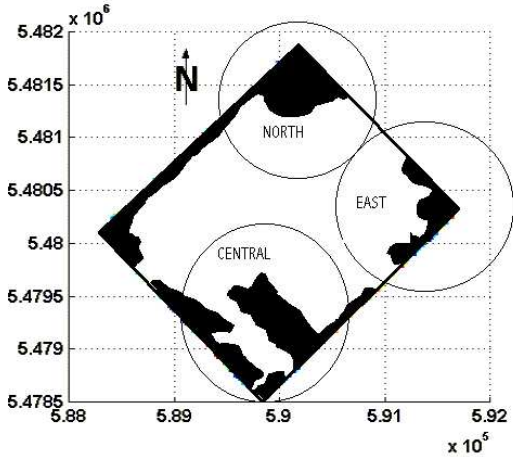


Fig. 1: Laterally heterogeneous areas in black, divided in sub-groups.

First, we estimate t_0 and V_{nmo} , by fitting the first two terms of equation (3). This estimate of V_{nmo} is compared to the one obtained by fitting in the least-square sense *all* offsets with equation (3). The latter technique also gives us estimates of V_{hor} and C . This shows that large offsets are needed to estimate ϵ as it is a function of the horizontal velocity. Both the fitting of small offsets and the complete suite of offsets are accompanied by a conservative error analysis and a sensitivity study.

Intermezzo: lateral homogeneity

Equation (3) holds for a laterally homogeneous medium. To study the lateral homogeneity of the overburden, we picked six horizons above the reservoir on the P-wave 3D surface seismic. The maps were converted to depth using the P-wave time-depth table from the near offset VSP. The regional dip is 0.5 degrees. We constructed five isopachs with a 95% confidence interval. Areas that were out of this interval were considered laterally heterogeneous, assuming the presence of lateral velocity variations or structural features (Figure 1). The boundaries of the survey are outside the interval as a result of poor surface seismic quality (low fold areas), but especially the area in the central region of the survey is suspect for lateral inhomogeneity. Later, we compare our parameter estimates with and without the sources in the regions of lateral inhomogeneity.

Near offsets

Figure 2 contains the squared travel times as a function of squared near offsets. Figure 3 shows V_{nmo} for the ten receivers as well as the corresponding δ parameter estimated from equation (1). The marker for each receiver is the estimate of V_{nmo} for the best fitting line through the data in Figure 2. However, the error bars are the result of fitting the dashed lines in Figure 2,

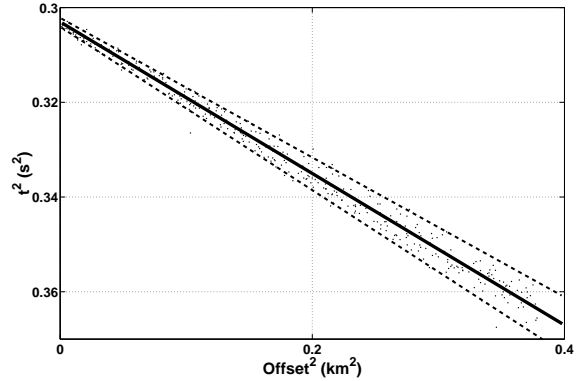


Fig. 2: Near offsets with a linear fit (solid line), the dashed lines represent the the deviations from the best fit. Receiver depth: 1232 m.

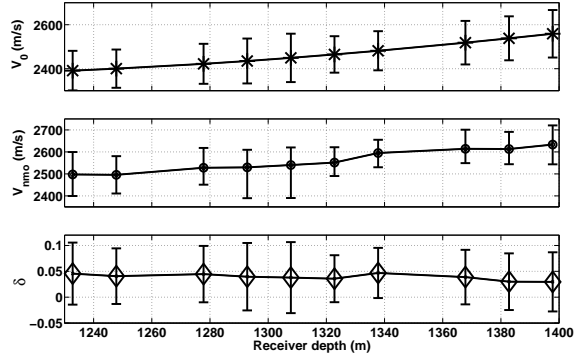


Fig. 3: Estimates of V_0 (top), V_{nmo} (middle) and δ (bottom) for ten receivers using only near offsets.

which contain the deviations from the best fit. The estimate and uncertainty in V_0 are from Adam (2001). The estimate of δ and its uncertainty are a direct result of propagation of errors in equation (1).

All offsets

Figure 4 shows the travel times for all offsets. The presence of isotropic layers and/or anisotropy within the layers produces the deviation from a straight line with increasing offset (Tsvankin, 2001). The overburden at Weyburn field shows this effect as a result of VTI anisotropy.

Here we invert for the governing parameters in equation (3) by a non-linear least squares approach. For this method, prior information involving lateral heterogeneity was used to study the sensitivity of the parameters (C , V_{nmo} , and V_{hor}) to areas that might behave laterally inhomogeneous (Figure 1). The errors shown in this section for V_{nmo} and V_{hor} are the worst case scenario of the inversion, as they include bias. For zero offset the error on the travel time is obtained from the regularized inversion of the near offset VSP (Adam, 2001). Far offset errors are estimated taking into account mis-picking, phase change and wavelet shape.

3D VSP travel time inversion in VTI media

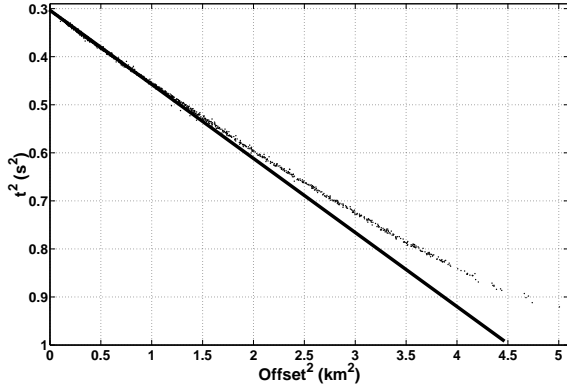


Fig. 4: Travel times for the receiver at 1232 m deviate from a straight line.

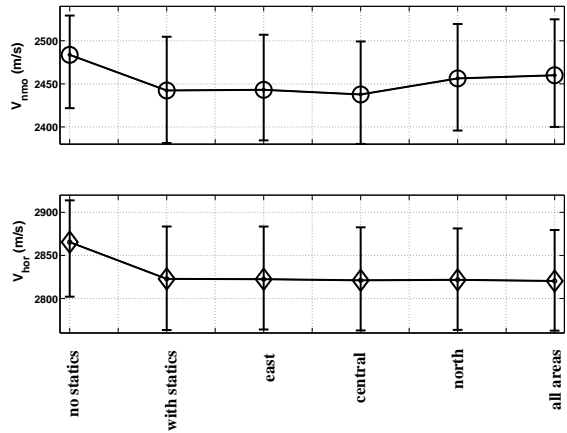


Fig. 5: Variation of NMO and horizontal velocities due to lateral heterogeneity. Receiver depth is 1337 m.

Figure 5 shows for the receiver at 1337 m the behavior of the V_{nmo} and V_{hor} without the sources from the areas of lateral heterogeneity. It can be seen that the NMO velocity has somewhat more variability to the areas than the horizontal velocity. The reason for this is that the objective function used in the non-linear inversion presents a flatter minimum for V_{nmo} than for V_{hor} . A flatter minimum means that there is a higher range of velocities that fit the data; therefore, a small variation is observed. We conclude that omitting sources in areas of possible lateral heterogeneities does not influence our estimates of anisotropic parameters, significantly.

Finally, Figure 6 shows the values of ϵ and δ for all the receiver depths using prior information lateral heterogeneity for all areas (even though it was not strictly necessary). When we compare the values of δ from the near offsets to the values from the non-hyperbolic moveout inversion, there is a difference in the magnitudes, and even more, in the sign. Non-hyperbolic moveout inversion has a trade-off between V_{nmo} and V_{hor} , which might produce the mismatch, while the near offsets only depend on V_{nmo} . A negative value of δ is more consistent with the geology of the area, as gamma-ray log shows that the overburden

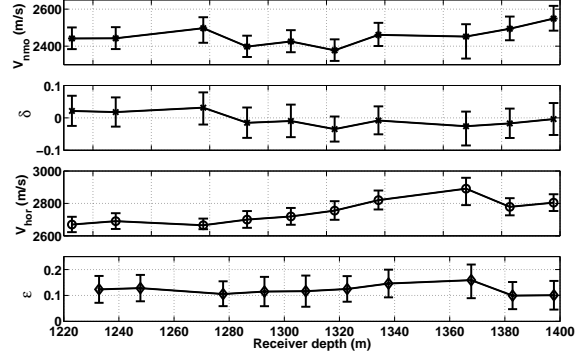


Fig. 6: Velocity and anisotropic parameter values for all depths, obtained using non-linear inversion of the travel times.

is composed of thin bedding, rather than a thick shale. As mentioned, the V_{nmo} obtained from the near offsets does not present a trade-off with V_{hor} . We use our estimate of V_{nmo} from near offsets into equation (3), and invert non-linearly, now only for V_{hor} . C is fixed to 0.5, this value is obtained from analysis described in the next section. These new estimate of V_{hor} if compared to the one inverted when using all three parameters, shows only 2% different in average. Therefore, the value of ϵ will not be significantly influenced if we have a small (10-100 m/s) variation in our V_{nmo} . The value of δ depends on V_{nmo} , thus its variation will affect the estimate of delta (Figures 3 and 6)

Sensitivity analysis

The sensitivity analysis consisted of changing one of the parameters by 20% in the non-hyperbolic moveout equation (t_0 , V_{nmo} , V_{hor} , C), while keeping the others with its estimated values. The vertical travel time variability showed to be the one that most influence the computed travel time.

Figure 6 shows the fit for different values of C . At short and intermediate offsets the fit is equivalent, but for the largest offsets the fit varies. Figure 8 shows the contours of travel time residuals for different pairs of V_{nmo} , V_{hor} , as we fix C . The resolution of the horizontal and NMO velocities is better for $C=0.5$, as the smallest contour gets tighter compared to the other two values of C . Another observation is the trade-off between V_{nmo} and V_{hor} . For $C \leq 0.5$, as V_{nmo} increases, V_{hor} increases. For a value of $C > 0.5$, as V_{nmo} increases, V_{hor} decreases. Although not shown in the Figure, negative values of C show multiple minima in the contours, suggesting different ranges of values for the velocities as optimal. Without other information, we do not wish to pick one minimum over the other. Either way, the range of velocities obtained due to different values of C is significant.

Conclusions

We estimate a range of possible values for ϵ and δ from

3D VSP travel time inversion in VTI media

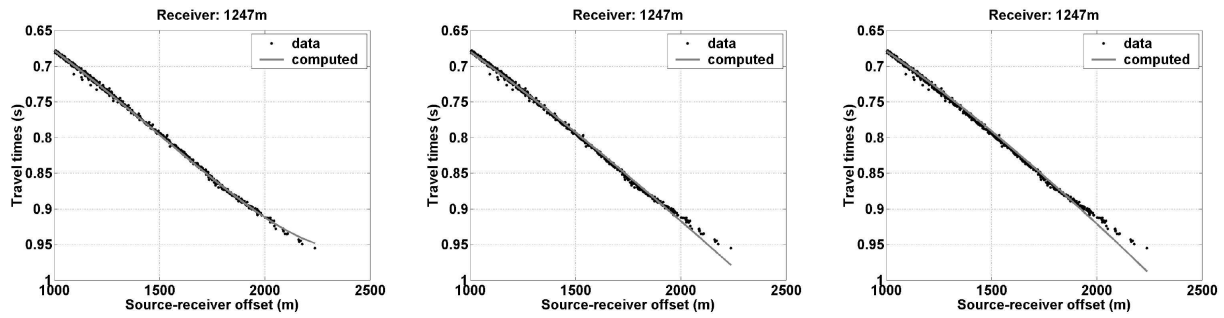


Fig. 7: Observed and predicted travel times for far offsets.

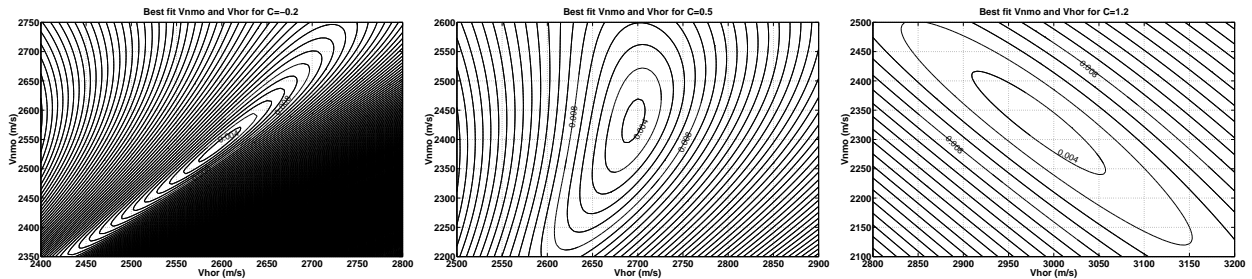


Fig. 8: Residual travel time contours for three values of C .

direct arrivals of a 3D VSP. Estimating δ using the non-hyperbolic moveout equation produces negative values, suggesting a thin-bedded overburden, instead of thick shale. Future work will include taking the vertical velocity gradient into account when inverting for anisotropic parameters.

Acknowledgments

We thank John Scales and Ilya Tsvankin for their discussion and the industry sponsors of the RCP and CWP.

References

- Adam, L., and Mattocks, B., 2002, Analysis of the 9C 3D VSP at Weyburn field: SOGV expanded abstracts.
- Adam, L., 2001, L-curve type inversion for error analysis for a near offset VSP: RCP Spring Sponsor Meeting Report.
- Grechka, V., and Tsvankin, I., 1998, Feasibility of non-hyperbolic moveout inversion in transversely isotropic media: *Geophysics*, **63**, 957–969.
- Thomsen, L., 1986, Weak elastic anisotropy: *Geophysics*, **51**, 1954–1966.
- Tsvankin, I., 2001, *Seismic signatures and analysis of reflection data in anisotropic media*: Elsevier Science, first edition.

Van Wijk, K., Scales, J. A., Navidi, W., and Tenorio, L., 2002, Data and model uncertainty estimation for linear inversion: *Geophys. J. Int.*, **149**, 625–632.

Wang, Z., 2002, Seismic anisotropy in sedimentary rocks, part 2: Laboratory data: *Geophysics*, **67**, 1423–1440.